

# Low-energy scattering and photoproduction of $\eta$ -mesons on three-body nuclei

A. Fix\* and H. Arenhövel

*Institut für Kernphysik, Johannes Gutenberg-Universität Mainz, D-55099 Mainz, Germany*

(Dated: October 31, 2018)

The optical potential approach for low-energy scattering of  $\eta$ -mesons on three-body nuclei is compared to an exact treatment of the  $\eta 3N$  system using four-body scattering theory with separable interactions in  $s$ -waves only. The higher-order terms including the interaction of the struck nucleon with the surrounding nuclear medium and virtual target excitations in between successive  $\eta$ -scatterings are found to cause important corrections. Effects of final state interaction in  $\eta$ -photoproduction on  ${}^3\text{H}$  and  ${}^3\text{He}$  are also studied and sizable contributions beyond the optical model approach are found.

PACS numbers: 13.60.-r, 13.75.-n, 21.45.+v, 25.20.-x

## I. INTRODUCTION

During the last 10 years much effort has been devoted to the study of the interaction of an  $\eta$ -meson with very light nuclei. The attention to this area, called primarily by the pioneering work of [1, 2], arises from the distinctive features of the  $\eta$ -nuclear system at low energies. In more detail:

(i) The  $\eta N$  interaction is characterized by the  $S_{11}(1535)$  resonance located near zero  $\eta N$  kinetic energy. As a consequence, the  $s$ -wave part of the  $\eta N$  interaction is attractive and rather large near threshold. This considerable attraction which is assumed to be coherently enhanced in nuclei has led to speculations about the existence of  $\eta$ -nuclear bound states which may be formed already in  $A = 3$  nuclei. Although a calculation using an energy independent  $\eta A$  potential has confirmed this hypothesis [2], more sophisticated investigations [3, 4] have shown that the  $\eta N$  interaction is unlikely to yield a bound  $\eta 3N$  system even with a relatively large real part of the scattering length  $\mathcal{R}e a_{\eta N} = 0.75$  fm. The pole of the scattering amplitude "recedes" to the nonphysical sheet generating an  $s$ -wave virtual state. It is important that apparently the pole is located close to the scattering threshold, resulting in a strong influence on low-energy scattering and production processes with  $\eta$ -mesons.

(ii) Concerning the formal aspects, the  $S_{11}(1535)$  resonance, dominating the low-energy  $\eta N$  interaction, must distort the transparent connection between the  $\eta N$  and  $\eta A$  scattering amplitudes. This connection is well established in the pion-nuclear case within the local-density limit where the equivalent optical potential is related in a simple fashion to the elementary  $\pi N$  amplitude [5] (except for real absorption of pions on few-nucleon clusters). The physical basis of this fact, giving rise to the so-called impulse approximation of the optical potential, is a large internucleon separation distance compared to the range of the  $\pi N$  interaction. On the contrary, due to the resonance pole in the  $\eta N$  interaction, the latter must be sizably influenced by the nuclear environment. Indeed, using  $\Gamma = 75$  MeV for the  $S_{11}(1535)$  width near the  $\eta N$  threshold, we obtain for the collision time  $\Delta t = 2\hbar/\Gamma \approx 1.7 \cdot 10^{-23}$  s which exceeds the time  $\Delta t = \hbar/m_\pi \approx 5 \cdot 10^{-24}$  s associated with the pion-exchange  $NN$  interaction. Therefore, the validity of the simplest optical potential for the  $\eta A$  interaction is expected to be doubtful, and more rigorous models have to be used.

The purpose of the present paper is to explore the interaction of  $\eta$ -mesons with three-body nuclei, a problem which can be solved exactly using methods developed within four-body scattering theory. At the same time, the generalization of the results obtained in this way to heavier nuclei seems to be more justifiable than in the deuteron case, where the two nucleons are strongly kinematically correlated and very weakly bound. Our intention is to analyze the quality of the first-order optical potential for the  $\eta 3N$  interaction using as a reference the exact four-body calculation. Since we have no way of direct fitting  $\eta$ -nuclear scattering cross sections using a phenomenological potential model, the information on the low-energy  $\eta$ -nuclear interaction stems entirely from the assumed properties of the  $\eta N$  interaction and depends strongly on the model linking these two processes. For this reason, a thorough microscopic approach to the  $\eta$ -nuclear dynamics becomes particularly important. On the other hand, rather complex mathematical infrastructure of the four-body scattering theory prevents to some extent a simple interpretation of the results. Therefore, we first will clarify the question, whether the  $\eta$ -nuclear interaction can be adequately described in terms of the simplest optical potential. Furthermore, the comparison of the four-body results with those obtained using less rigorous but very tractable approaches, such as the lowest-order optical potential, may be very fruitful in

---

\* On leave of absence from Tomsk Polytechnic University, 634034 Tomsk, Russia

understanding the  $\eta 3N$  interaction mechanism.

Several aspects concerning the accuracy of the simplest optical model for the scattering of  $\eta$  mesons on  $s$ -shell nuclei were already discussed in Ref. [3]. In particular, it was shown that the behavior of the  $\eta N$  scattering matrix below the free threshold has a crucial influence on the results. Here we address other questions related to the optical potential approach for  $\eta 3N$  scattering, namely:

- (i) What is the influence of binding of the participating nucleon on the elementary scattering process?
- (ii) What is the relative importance of target excitations in between two successive scatterings on different nucleons?
- (iii) What is the importance of the short-range behavior of the nucleon-nucleon potential?

The second part of the paper is devoted to coherent  $\eta$ -photoproduction on three-body nuclei



These reactions are of special importance in  $\eta$ -nuclear physics. Firstly, the main driving mechanism of  $\eta$ -photoproduction, the photoexcitation of the  $S_{11}(1535)$ -resonance, is well established. This is in contrast to reactions with nucleons as incident particles, where the main mechanism connected with the short-range part of the  $NN$  interaction is presumably much more complex and as of yet not well understood. Secondly, the energy gap between the coherent and incoherent thresholds, where the  $\eta$ -yield is free from the strong incoherent background is about  $\Delta E_\gamma = 7$  MeV, which is appreciably larger than the one on the deuteron (about 3 MeV). This advantage has been partially used in a recent  ${}^3\text{He}(\gamma, \eta){}^3\text{He}$  experiment carried out with the TAPS facility operating at MAMI [6]. Thirdly, the  $\eta$ -nuclear interaction, which is most important in the  $s$ -wave, must be particularly significant in reactions involving nuclei with nonzero spin. As a counter example, the reaction  ${}^4\text{He}(\gamma, \eta){}^4\text{He}$ , where the  $s$ -wave in the final state is totally suppressed, does not show any strong influence of the final state interaction (FSI). Finally, the dynamics of the reactions (1) may be treated within a few-body scattering theory, i.e., formally exactly. Though the near-threshold  $\eta$ -photoproduction on three-body nuclei was already considered in Ref. [7] within the so-called finite-rank-approximation (FRA), we reexamine it primarily in order to show the results of the four-body approach for the  $\eta 3N$  interaction in the final state.

The outline of the paper is as follows. First, we briefly review in Sect. II the four-body formalism which is relevant for the present consideration. For the separable representation of the kernels we use the energy dependent pole expansion (EDPE) method of Ref. [8]. In Sect. III, after a short summary of the Kerman-McManus-Thaler (KMT) theory, we discuss the "standard" optical model for the  $\eta 3N$  elastic scattering with particular emphasis on the role of the higher-order corrections like nucleon-core interaction and virtual target excitations. The  $\eta$ -photoproduction on three-body nuclei is presented in Sect. IV where we illustrate the strong effect of the  $\eta 3N$  interaction in the final state. In this section we also compare our predictions with those given in [7]. The main results are reviewed in the conclusions.

## II. THE FOUR-BODY APPROACH TO $\eta 3N$ SCATTERING

We begin the formal part with a brief review of the four-body scattering formalism applied to  $\eta 3N$  scattering. Our basic tool for solving the four-body equations is the quasiparticle method, reduced to a purely separable representation for the driving two-body potentials and also for the subamplitudes in the (3+1) and (2+2) partitions. The main features of the method were widely presented in the literature (see e.g. Ref. [9] and references therein). In applying this approach to the  $\eta 3N$  problem, the relevant formalism is considered in [4]. Within the quasiparticle method, the whole dynamics is described in terms of the amplitudes  $X_{\alpha 1}$  ( $\alpha=1,2,3$ ) connecting the three quasi-two-body channels characterized by the following partitions

$$\alpha = 1 : \eta + (3N), \quad \alpha = 2 : N + (\eta NN), \quad \alpha = 3 : (\eta N) + (NN) \quad (2)$$

with the initial channel  $\alpha=1$ . To be specific, we consider the triton as target. Because we neglect coulomb forces and thus isospin invariance holds, the channels with  ${}^3\text{H}$  and  ${}^3\text{He}$  are identical. Since only the energies up to the three-body threshold will be considered, we treat the pion energy relativistically but use nonrelativistic kinematics for nucleons and the  $\eta$ -meson. Furthermore, due to strong dominance of  $s$ -waves in  $NN$  and  $\eta N$  scattering, we assume that in the low-energy region only the lowest partial wave ( $L=0$ ) in the  $\eta 3N$  system has to be taken into account.

The essence of the calculational scheme is the solution of the scattering problem for the two- and three-body subsystems specified in the partitions (2). For  $\alpha = 1$  and 2 we deal with interacting three-body systems. Using separable representations for the  $NN$  and  $\eta N$  potentials, the corresponding scattering amplitudes can be expressed in terms of effective quasi-two-body amplitudes  $U_{\alpha;ij}(q, q'; \mathcal{E})$  which describe the scattering of a particle on a two-body cluster (quasiparticle). The corresponding states are specified by the indices  $i, j$  marking the quasiparticles, e.g.,  $i, j \in \{d, N^*\}$  for  $\alpha = 2$  where the  $(NN)$  and  $(\eta N)$  systems are denoted as  $d$  and  $N^*$ , respectively. The notation

$N^*$  is associated with the  $S_{11}(1535)$  resonance which dominates the low energy  $\eta N$  interaction. For  $\alpha = 3$  we have two independent two-particle subsystems. The relevant amplitudes are also represented in the quasi-two-body form  $U_{3;ij}(q, q'; \mathcal{E})$  with  $i, j \in \{d, N^*\}$  [4].

The reduction of the four-body equations to a numerically manageable form is achieved by expanding the amplitudes  $U_{\alpha;ij}$  into separable series of finite rank  $N_\alpha$

$$U_{1;dd}^{(ss')} (q, q'; \mathcal{E}) = \sum_{l,m=1}^{N_1} v_{d;l}^{1(s)}(q; \mathcal{E}) \Theta_{1;lm}(\mathcal{E}) v_{d;m}^{1(s')}(q'; \mathcal{E}), \quad (3)$$

$$U_{\alpha;ij}^{(s)} (q, q'; \mathcal{E}) = \sum_{l,m=1}^{N_\alpha} v_{i;l}^{\alpha(s)}(q; \mathcal{E}) \Theta_{\alpha;lm}^{(s)}(\mathcal{E}) v_{j;m}^{\alpha(s)}(q'; \mathcal{E}), \quad \alpha = 2, 3. \quad (4)$$

To condense the formulas to follow, we use here a unified notation for the vertex functions or form factors  $v^\alpha$  in all three channels. They are related to the ones introduced in [4] as:  $v_{d;n}^1 = u_n$ ,  $v_{i;n}^2 = v_{i;n}$ ,  $v_{i;n}^3 = w_{i;n}$ ,  $i \in \{d, N^*\}$ . For the sake of clarity, we note that the amplitude  $U_1$  of the  $(NN) + N$  scattering is a  $2 \times 2$  matrix according to the spin index  $s = 0, 1$  (we need only spin-doublet  $3N$  states). Here the values  $s = 0, 1$  denote the total spin of the  $(NN)$   $s$ -wave cluster with isospin  $t = 1 - s$ . At the same time, in the partitions  $\alpha = 2, 3$ , we have two one-dimensional amplitudes  $U_\alpha^{(s)}$ . For instance, in the channel  $\alpha = 2$  the index  $s$  numerates two independent  $\eta NN$  states with  $J^\pi = 0^-$  ( $s=0$ ) and  $J^\pi = 1^-$  ( $s=1$ ), respectively.

Considering the identity of the nucleons, the  $\eta 3N$  problem is reduced to a  $3 \times 3$  set of integral equations in one scalar variable. For the transition amplitudes  $X_{\alpha 1}$  connecting the channel 1 to the channels  $\alpha = 2$  and 3 we arrive at a coupled set of equations

$$X_{\alpha 1;nn'}^{(ss')} (p, p'; E) = Z_{\alpha 1;nn'}^{(ss')} (p, p'; E) + \sum_{\beta=2,3} \sum_{l,m} \sum_{\sigma=0,1} \int_0^\infty \tilde{Z}_{\alpha\beta;nl}^{(\sigma)}(p, p''; E) \Theta_{\beta;lm}^{(\sigma)} \left( E - \frac{p''^2}{2M_\beta} \right) X_{\beta 1;mn'}^{(\sigma s')} (p'', p'; E) \frac{p''^2 dp}{2\pi^2}, \quad \alpha = 2, 3, \quad (5)$$

where  $Z_{\alpha\beta}$  and  $\tilde{Z}_{\alpha\beta}$  are the effective potentials realized through particle exchange between the quasiparticles in the channels  $\alpha$  and  $\beta$ . The arguments of the effective propagators  $\Theta_\alpha$  are the internal energies of the corresponding clusters, given in (2). In the case  $\alpha = 3$  it is equal to the sum of the c.m. kinetic energies in the  $\eta N$  and  $NN$  subsystems. The reduced masses in the three channels read

$$M_1 = \frac{3M_N m_\eta}{3M_N + m_\eta}, \quad M_2 = \frac{M_N(2M_N + m_\eta)}{3M_N + m_\eta}, \quad M_3 = \frac{2M_N(M_N + m_\eta)}{3M_N + m_\eta}. \quad (6)$$

The equations (5) are illustrated in Fig. 1, where also the structure of the potentials  $Z_{\alpha\beta}$  and  $\tilde{Z}_{\alpha\beta}$  is schematically explained. The former are expressed in terms of the form factors  $v_{i;n}^\alpha$  as

$$Z_{\alpha\beta;nn'}^{(ss')} (p, p'; E) = \frac{\Omega_{ss'}}{2} \sum_j \int_{-1}^{+1} v_{j;n}^{\alpha(s)}(q, E - \frac{p^2}{2M_\alpha}) \tau_j^{(s)} \left( E - \frac{p^2}{2M_\alpha} - \frac{q^2}{2\mu_j^\alpha} \right) v_{j;n'}^{\beta(s')}(q', E - \frac{p'^2}{2M_\beta}) d(\hat{p} \cdot \hat{p}'). \quad (7)$$

Here, the functions  $\tau_j(z)$  are the familiar quasiparticle propagators appearing in the separable model for  $NN$  ( $j = d$ ) and  $\eta N$  ( $j = N^*$ ) scattering which depend on the two-body c.m. kinetic energies. The corresponding reduced masses  $\mu_j^\alpha$  read

$$\mu_d^1 = \frac{3}{2}M_N, \quad \mu_d^2 = \frac{2M_N m_\eta}{2M_N + m_\eta}, \quad \mu_{N^*}^2 = \frac{M_N(M_N + m_\eta)}{2M_N + m_\eta}, \quad \mu_d^3 = \frac{M_N m_\eta}{M_N + m_\eta}, \quad \mu_{N^*}^3 = \frac{M_N}{2}. \quad (8)$$

The spin-isospin coefficients are denoted by  $\Omega_{ss'}$ . Clearly, due to the pseudoscalar-isoscalar nature of the  $\eta$  meson the spin  $s$  of the  $NN$ -cluster fixes uniquely the order of the spin-isospin coupling of the whole  $\eta 3N$  configuration. The momenta  $q$  and  $q'$  in (7) are functions of the variables  $\vec{p}, \vec{p}'$  and  $E$  as given in [4]. The overall c.m. energy  $E$  is counted from the four-body threshold, i.e.  $E = W - 3M_N - m_\eta$  with  $W$  being the  $\eta^3\text{H}$  invariant mass. Below the first inelastic threshold the obvious relation  $E \leq -\varepsilon_d$  holds, where  $\varepsilon_d$  denotes the deuteron binding energy. For more details concerning the structure of the potentials  $\tilde{Z}_{\alpha\beta}$  and  $Z_{\alpha\beta}$  we refer to Ref. [4].

Elastic  $\eta^3\text{H}$  scattering is described by the amplitude  $X_{11}$ , which is determined by the amplitudes  $X_{\alpha 1}$  ( $\alpha = 2, 3$ ) as

$$X_{11;nn'}^{(ss')}(p, p'; E) = \sum_{\alpha=2,3} \sum_{l,m} \sum_{\sigma=0,1} \int_0^\infty Z_{1\alpha;nl}^{(s\sigma)}(p, p''; E) \Theta_{\alpha;lm}^{(\sigma)}\left(E - \frac{p''^2}{2M_\beta}\right) X_{\alpha 1;mn'}^{(\sigma s')}(p'', p'; E) \frac{p''^2 dp}{2\pi^2}. \quad (9)$$

As was already mentioned, the key point of the reduction procedure, leading to numerically manageable equations (5), is the separable expansion of the subamplitudes (3) and (4). In the present paper we use for this purpose the method of the energy dependent pole expansion (EDPE), presented in detail in [8]. The starting point is the eigenvalue equation for the vertex functions  $v_{i;n}^\alpha(q, \mathcal{E})$

$$v_{d;n}^{1(s)}(q, B_1) = \frac{1}{\lambda_n^1} \sum_{s'=0,1} \int_0^\infty V_{1;dd}^{(ss')}(q, q'; B_1) \tau_d^{(s')}(B_1 - \frac{q'^2}{2\mu_d^1}) v_{d;n}^{1(s')}(q', B_1) \frac{q'^2 dq'}{2\pi^2}, \quad (10)$$

$$v_{i;n}^{\alpha(s)}(q, B_\alpha) = \frac{1}{\lambda_n^{\alpha(s)}} \sum_{j=d, N^*} \int_0^\infty V_{\alpha;ij}^{(s)}(q, q'; B_\alpha) \tau_j^{(s)}(B_\alpha - \frac{q'^2}{2\mu_j^\alpha}) v_{j;n}^{\alpha(s)}(q', B_\alpha) \frac{q'^2 dq'}{2\pi^2}, \quad \alpha = 2, 3. \quad (11)$$

The explicit expressions for the effective potentials  $V_{\alpha;ij}(q, q'; \mathcal{E})$  are given in Ref. [4]. The equations (10) are solved for an arbitrarily fixed energy  $\mathcal{E} = B_\alpha$ . In the actual calculation we have taken  $B_1 = -\varepsilon_{3H}$  (the triton binding energy) and  $B_\alpha = -\varepsilon_d$  in the other two channels  $\alpha = 2, 3$ .

The extrapolation of the vertices  $v_{i;n}^\alpha$  onto the whole energy axes is carried out according to the expressions

$$v_{d;n}^{1(s)}(q, \mathcal{E}) = \sum_{s'=0,1} \int_0^\infty V_{1;dd}^{(ss')}(q, q'; \mathcal{E}) \tau_d^{(s')}(B_1 - \frac{q'^2}{2\mu_d^1}) v_{d;n}^{1(s')}(q', B_1) \frac{q'^2 dq'}{2\pi^2}, \quad (12)$$

$$v_{i;n}^{\alpha(s)}(q, \mathcal{E}) = \sum_{j=d, N^*} \int_0^\infty V_{\alpha;ij}^{(s)}(q, q'; \mathcal{E}) \tau_j^{(s)}(B_\alpha - \frac{q'^2}{2\mu_j^\alpha}) v_{j;n}^{\alpha(s)}(q', B_\alpha) \frac{q'^2 dq'}{2\pi^2}, \quad \alpha = 2, 3. \quad (13)$$

The effective EDPE propagators  $\Theta_\alpha$  in (3) and (4) are defined by

$$(\Theta_1^{-1}(\mathcal{E}))_{mn} = \sum_{s=0,1} \int_0^\infty [v_{d;m}^{1(s)}(q, B_1) \tau_d^{(s)}(B_1 - \frac{q^2}{2\mu_d^1}) - v_{d;m}^{1(s)}(q, \mathcal{E}) \tau_d^{(s)}(\mathcal{E} - \frac{q^2}{2\mu_d^1})] v_{d;n}^{1(s)}(q, \mathcal{E}) \frac{q^2 dq}{2\pi^2}, \quad (14)$$

$$(\Theta_\alpha^{(s)-1}(\mathcal{E}))_{mn} = \sum_{j=d, N^*} \int_0^\infty [v_{j;m}^{\alpha(s)}(q, B_\alpha) \tau_j^{(s)}(B_\alpha - \frac{q^2}{2\mu_j^\alpha}) - v_{j;m}^{\alpha(s)}(q, \mathcal{E}) \tau_j^{(s)}(\mathcal{E} - \frac{q^2}{2\mu_j^\alpha})] v_{j;n}^{\alpha(s)}(q, \mathcal{E}) \frac{q^2 dq}{2\pi^2}, \quad \alpha = 2, 3. \quad (15)$$

In the calculation, we use a  $6 \times 6$  separable representation (3) and (4) in each partition (2) which yields accurate solutions up to the first inelastic threshold.

Due to the strong coupling between the  $\eta N$  and  $\pi N$  channels in the  $S_{11}(1535)$  region, the transitions  $\eta N \leftrightarrow \pi N$  must in general be taken into account. Clearly, the most straightforward way to introduce the pion degrees of freedom would be to generalize the  $\eta 3N$  four-body equations to include the coupled channels ( $\pi 3N$ )  $\leftrightarrow$  ( $\eta 3N$ ). But in practice, the four-body treatment of the  $\pi 3N$  states turns out to be very complicated. The reason for this is the appearance of moving singularities arising near the physical region for the  $\pi NN$  amplitudes above the three-body threshold. As a result, the separable representation of the four-body kernels converges very poorly [10]. Therefore, we neglect the channel  $\pi 3N$  keeping only the intermediate  $\pi N$ -”bubbles” in the  $S_{11}(1535)$  propagator. The validity of this neglect seems to be doubtful, since the  $\pi N$  interaction in the second resonance region is visibly stronger than the  $\eta N$  one. The crucial point, however, is that the two-step process  $\eta N \rightarrow \pi N \rightarrow \eta N$ , favoring large momenta of the intermediate pion  $k_\pi \approx 400$  MeV/c, needs two nucleons to be within the range  $R = \hbar/k_\pi \approx 0.5$  fm. Adopting a simple geometric interpretation, the corresponding mechanism is associated with a small probability

$$P = \frac{4}{3} \pi R^3 \rho_{3H}(0) \approx \frac{1}{10}, \quad (16)$$

where  $\rho_{3H}(r)$  is the  $^3\text{H}$  nucleon density, and thus is not expected to be effective for low-energy  $\eta^3\text{H}$  scattering.

For the target wave function we take only the  $s$ -wave part

$$\Psi_{M_J M_T}(\vec{q}, \vec{k}) = \frac{1}{\sqrt{3}} (1 - P_{12} - P_{13}) \sum_{s=0,1} \psi^{(s)}(q_1, k_{23}) \left[ \left[ \frac{1}{2} \times \frac{1}{2} \right]^{st} \times \frac{1}{2} \right]^{\frac{1}{2} M_J \frac{1}{2} M_T}, \quad (17)$$

where the isospin  $t = 1 - s$  and  $M_J$  and  $M_T$  denote total spin and isospin projections, respectively. The spatial functions  $\psi^{(s)}(q_1, k_{23})$  are taken symmetric with respect to the nucleons 2 and 3. They are extracted from the bound state pole of the  $3N$  scattering amplitude, calculated within the three-body model. The corresponding expression in terms of the  $(3N) \rightarrow N + (NN)$  vertices  $v_{d;1}^{1(s)}$  reads

$$\psi^{(s)}(q, k) = -N g_d^{(s)} \tau_d^{(s)} \left( -\varepsilon_{3H} - \frac{3q^2}{4M_N} \right) \frac{v_{d;1}^{1(s)}(q, -\varepsilon_{3H})}{\varepsilon_{3H} + \frac{3q^2}{4M_N} + \frac{k^2}{M_N}}. \quad (18)$$

The normalization factor is obtained from the residue of the scattering matrix

$$N^{-2} = \left. \frac{d\lambda_1^1}{d\mathcal{E}} \right|_{\mathcal{E} = -\varepsilon_{3H}}, \quad (19)$$

where  $\lambda_1^1$  is the first eigenvalue of the kernel  $V_{1;dd}\tau_d$  (see Eq. (10)). Finally, for the  $\eta^3\text{H}$  scattering amplitude we get

$$F_{\eta^3\text{H}}(k_\eta) = -\frac{\mu_{\eta^3\text{H}}}{2\pi} \sum_{s,s'=0,1} X_{11;11}^{(ss')}(k_\eta, k_\eta; E), \quad (20)$$

with the  $\eta^3\text{H}$  reduced mass  $\mu_{\eta^3\text{H}}$  and the on-shell momentum  $k_\eta = [2\mu_{\eta^3\text{H}}(E + \varepsilon_{3H})]^{1/2}$ .

As was already noted, we consider the  $NN$  and  $\eta N$  interactions only in  $s$  states. For the  $NN$   $^1S_0$  and  $^3S_1$  configurations we adopt a rank-one separable parametrization

$$v_{NN}^{(s)}(k, k') = -g_d^{(s)}(k)g_d^{(s)}(k'), \quad \text{with } g_d^{(s)}(k) = \sqrt{2}\pi \sum_{i=1}^6 \frac{C_i^{(s)}}{k^2 + \beta_i^{(s)2}}, \quad \text{for } s = 0, 1, \quad (21)$$

where the parameters  $C_i^{(s)}$  and  $\beta_i^{(s)}$  are listed in Ref. [11]. The index  $s = 0, 1$  refers to the singlet and triplet states, respectively. The separable potential (21) is obtained by fitting the off-shell behavior of the Paris  $NN$  potential at zero energy and is therefore appropriate for processes without target break-up. The corresponding three-body calculation gives for the triton binding energy a reasonable value  $\varepsilon_{3H} = 8.64$  MeV and describes rather well the  $^3\text{H}$  charge form factor up to  $Q^2 = 8 \text{ fm}^{-2}$ .

As for the  $\eta N$  interaction, we use here the simplest separable parametrization with the energy-dependent potential

$$v_{\eta N}(k, k'; W) = \frac{g_{N^*}^{(\eta)}(k)g_{N^*}^{(\eta)}(k')}{W - M_0}, \quad \text{with } g_{N^*}^{(\eta)}(k) = \frac{g_{N^*}^{(\eta)}}{\sqrt{2}\omega_\eta} \frac{\beta_{N^*}^{(\eta)2}}{k^2 + \beta_{N^*}^{(\eta)2}}, \quad (22)$$

which gives the familiar isobar ansatz for the meson-nucleon amplitude with the bare resonance mass  $M_0$ . In the present paper, the excitation of the  $S_{11}(1535)$  resonance is assumed to be the only mechanism for the meson-nucleon interaction. Rather than to investigate the dependence of the results on the  $\eta N$  scattering length  $a_{\eta N}$  we preferred to choose the parameters in (22) such that the  $\eta N$  scattering length

$$a_{\eta N} = (0.50 + i0.32) \text{ fm} \quad (23)$$

is reproduced. This value lies approximately "halfway" in the listing of various  $\eta N$  scattering lengths which can be found in the literature (see e.g. [12]). It must be noted that the low-energy  $\eta$ -nuclear interaction depends strongly on the continuation of the  $\eta N$  amplitude to negative kinetic energies and hence must be sensitive to the amplitudes in the channels coupled to the  $\eta N$  one. Therefore, we use here the unitary model of Ref. [13] where three coupled channels  $\eta N$ ,  $\pi N$  and  $\pi\pi N$  are considered. In order to reproduce the value (23) we have slightly changed the set of parameters presented in [13] in such a manner that the  $\pi N \rightarrow \pi N$  and  $\pi N \rightarrow \eta N$  scattering data are reasonably well described in the region below and just above the  $\eta N$  threshold. The results shown in Fig. 2 are obtained with the parameter values

$$\begin{aligned} g_{N^*}^{(\pi)} &= 8.898/\sqrt{12\pi}, & \beta_{N^*}^{(\pi)} &= 404 \text{ MeV}, \\ g_{N^*}^{(\eta)} &= 7.090/\sqrt{4\pi}, & \beta_{N^*}^{(\eta)} &= 695 \text{ MeV}, \\ M_0 &= 1599 \text{ MeV}. \end{aligned} \quad (24)$$

The additional factors in (24) appear due to different normalizations of the meson-nucleon potentials  $v_{\pi N}$  and  $v_{\eta N}$  used in this work and in [13]. The parameters of the two-pion channel  $\pi\pi N$  were taken unchanged from Ref. [13].

### III. THE OPTICAL MODEL FOR $\eta^3\text{H}$ SCATTERING

We begin the analysis of the optical potential approach by reviewing the corresponding formalism. According to the Watson multiple scattering theory [16], the  $\eta$ -nuclear interaction may be treated as a series of  $\eta N$  collisions. In the present discussion we use the version put forward by Kerman-McManus-Thaler (KMT) [17]. The corresponding expansion of the scattering operator reads

$$T = \sum_i^A \tau(i) + \sum_{i \neq j}^A \tau(i)G\tau(j) + \dots \quad (25)$$

Here the Green's function  $G$  describes the propagation of a free  $\eta$  and  $A$  interacting nucleons

$$G = \frac{\hat{A}}{E - H_0 - V_A}, \quad (26)$$

where the nuclear potential  $V_A$  describes the interactions of the nucleons, and the free Hamiltonian  $H_0$  includes only the kinetic energy operator of meson and nucleons. Furthermore, we have included into the Green's function the projection operator  $\hat{A}$  onto the completely antisymmetric nuclear states. The scattering matrix  $\tau$  in (25) describes the off-shell scattering of an  $\eta$ -meson on a single bound nucleon and obeys the equation

$$\tau = v_{\eta N} + v_{\eta N}G\tau. \quad (27)$$

Within the KMT theory the nucleons are treated to be identical from the beginning. Therefore we have dropped the nucleon index  $i$  in (27). The formal reduction of the  $(A+1)$ -body problem (25)-(27) to a two-body scattering problem leads for the  $T$ -matrix to the equation

$$T = U + \frac{A-1}{A} UGP_0T, \quad (28)$$

with  $P_0$  being the projector onto the nuclear ground state. The operator  $U$  of the equivalent optical potential obeys the equation

$$U = U^{(1)} + \frac{A-1}{A} U^{(1)}G(1 - P_0)U, \quad (29)$$

with the driving term  $U^{(1)} = A\tau$ .

The simplest realization of the multiple scattering formalism is mainly based on the following approximations:

(i) Coherent approximation: here one keeps only the leading term in (29). The resulting optical potential is given by the the ground state expectation value of the matrix  $\tau$  times the number of nucleons in the nucleus

$$U_C(\vec{p}, \vec{p}'; E) = \langle 0; \vec{p} | U^{(1)}(E) | 0; \vec{p}' \rangle = A \langle 0; \vec{p} | \tau | 0; \vec{p}' \rangle. \quad (30)$$

As may be seen, the restriction to the first-order term  $U^{(1)}$  in the expansion (29) neglects the virtual target excitations in between successive scatterings on different nucleons. Of course, as follows from (27), excitations are allowed for when the  $\eta$  interacts successively with the same nucleon. One of the points in favor of the coherent approximation is the assumed dominance of the nearest singularity (bound state pole). Probably no less important is the orthogonality of the nuclear ground state wave function to the excited states, which results in a reduction of the matrix element  $\langle 0 | U^{(1)} | n \rangle$  at least at small momentum transfers. However, in spite of these reasonable arguments the study of  $nd$  [18] and  $\eta d$  [19] scattering has shown that keeping only the target ground state weakens sizably the overall interaction in the system and is therefore a rather poor approximation.

(ii) Impulse approximation: it is considered as a further simplification of the approximation (i) and consists in the substitution of the operator  $\tau$  in (30) by the free-space  $\eta N$  scattering matrix  $t_{\eta N}$  satisfying the equation

$$t_{\eta N} = v_{\eta N} + v_{\eta N}G_0t_{\eta N}, \quad \text{with } G_0 = \frac{1}{E - H_0}. \quad (31)$$

The resulting optical potential for the  $\eta^3\text{H}$  scattering is then

$$U_I(\vec{p}, \vec{p}'; E) = A \langle 0; \vec{p} | t_{\eta N} | 0; \vec{p}' \rangle = A \int \Psi_{3H}^*(\vec{q}, \vec{k}) t_{\eta N}(w_{\eta N}(\vec{q})) \Psi_{3H}(\vec{q} + \frac{2}{3}(\vec{p} - \vec{p}'), \vec{k}) \frac{d^3q}{(2\pi)^3} \frac{d^3k}{(2\pi)^3}, \quad (32)$$

where the argument  $\vec{q}$  of the ground state wave function  $\Psi_{3H}$  is the relative momentum of the participating nucleon with respect to the other two nucleons. Thus within this approximation, the struck nucleon is bound only before and after the interaction with the incident meson but is free during the scattering. The role of the surrounding nucleons is to provide only the momentum distribution for the active scatterer. The impulse approximation is more or less successful for low-energy pion-nucleus scattering far away from the resonance region [5], that is, for light projectiles which interact weakly with the target constituents. But its validity may be marginal in the  $\eta$ -nuclear case. The main reason for this fact is that the impulse approximation breaks down if the projectile is in resonance with the nucleon [16]. As was already noted in the introduction, since the  $\eta N$ -scattering is associated with a nonvanishing time delay due to the  $S_{11}(1535)$  resonance, the interaction of the struck nucleon with the remaining ones must generally be important.

In order to study the quality of the approximations (i) and (ii) for the  $\eta$ -nuclear interaction we have calculated the  $\eta^3\text{H}$  elastic scattering using the optical potentials  $U_C$  (30) and  $U_I$  (32). In each case only the  $s$ -wave part of the scattering amplitude was taken into account. The results are obtained by solving equation (28) in momentum space

$$T(p, p'; E) = U(p, p'; E) + \frac{2}{3} \frac{\mu_{\eta^3H}}{\pi^2} \int_0^\infty \frac{U(p, p'; E) T(p', p; E)}{p^2 - p'^2 + i\varepsilon} p'^2 dp'. \quad (33)$$

The numerical difficulties caused by the singularity in the integrand at  $p' = p$  were eliminated with the help of the Noyes-Kowalski trick [20].

It is worthwhile to note that since the in-medium  $\eta N$  scattering matrix  $\tau$  is an  $(A + 1)$ -body operator, its full treatment is in general possible only with certain approximations. However, in the case of  $A = 3$ , the equation (27) can be solved exactly using the four-body formalism. Indeed, this equation represents the reduced problem where the  $\eta$ -meson is scattered off only one of the nucleons which in turn interacts with the other two nucleons. Therefore, using the separable representation for the two- and three-body scattering matrices as described in Sect. II, the equation (27) can be transformed into the form presented in (5) and (9) where now we must switch off the  $\eta$  exchange between the nucleons. In the computation, we simply set the potential  $V_{2;N^*N^*}$  in Eqs. (11) and (13) as well as the term  $Z_{23}^1(Z_{32}^1)$  in the potential  $\tilde{Z}_{23}(\tilde{Z}_{32})$  (see Fig. 1) equal to zero. The matrix  $X_{11}$ , obtained in this way, yields the  $s$ -wave potential  $U_C$  (30) for the  $\eta^3\text{H}$  scattering in the form

$$U_C(p, p'; E) = \sum_{ss'=0,1} X_{11;11}^{(ss')} (p, p'; E). \quad (34)$$

In Fig. 3 we compare the results of the approximations (30) and (32) with those given by the four-body theory where the  $\eta 3N$  multiple scattering series (25) is summed exactly. There are two main conclusion to be drawn from this comparison:

(i) The  $\eta^3\text{H}$  interaction generated by the optical potential  $U_I$  (32) is relatively weak. It is interesting to compare our result with that obtained within the scattering length approximation  $t_{\eta N} \rightarrow -\frac{2\pi}{\mu_{\eta N}} a_{\eta N}$ . The latter predicts a binding of the  $\eta 3N$  system already for relatively modest values of  $a_{\eta N}$  (see e.g. [2, 21]). The trivial source of this discrepancy lies in the strong energy dependence of the  $\eta N$  amplitude which is ignored by the scattering length approximation. The change of the free  $\eta N$  energy  $w_{\eta N}^{\text{free}}$  in the medium is primarily due to the Fermi motion and due to the binding of the nucleons. A rough estimation at zero  $\eta^3\text{H}$  kinetic energy gives

$$\Delta\omega = w_{\eta N} - w_{\eta N}^{\text{free}} \approx -\varepsilon_b - \frac{\langle q^2 \rangle}{2M_3}, \quad (35)$$

where  $\varepsilon_b \approx 6.5$  MeV is the binding energy of a participating nucleon to the two-nucleon core, while  $\langle q^2 \rangle$  stands for the mean squared nucleon momentum inside the nucleus, and the reduced mass  $M_3$  is given by (6). Taking  $\sqrt{\langle q^2 \rangle} = 120$  MeV/c we obtain  $\Delta\omega \approx -15$  MeV. In the calculation, the energy at which the  $\eta N$  amplitude has to be calculated was chosen according to the so-called "spectator on-shell" prescription. The corresponding energy shift  $|\Delta\omega|$  is larger than that given by the estimation (35) where the internal energy of the two-nucleon core is neglected. Taking into account the difference  $\Delta\omega$  results in decreasing the  $\eta N$  scattering amplitude and especially its imaginary part, which has a sharp energy dependence around the  $\eta N$  threshold (see Fig. 2). The crucial importance of this fact was also discussed in [3, 12]. One sees in Fig. 3 that inclusion of the intermediate nuclear interaction (the dash-dotted curve)

accounts for an appreciable portion of the noted disagreement, and it leads to a much better description near zero energy. We consider this fact as evidence that calculations, which investigate the dependence of the  $\eta A$ -dynamics on the elementary amplitude  $t_{\eta N}$  but disregard the interaction of the participating nucleon with the surrounding nucleons, are of little significance.

(ii) Comparison of the results obtained within the coherent approximation (30) with the four-body treatment shows the role of higher order terms in the expansion (29). As was already noted, their contribution is associated with virtual target excitations in between scatterings. As one sees, this effect is significant and increases as the energy approaches the inelastic threshold (analogous conclusions with respect to the  $\eta d$  interaction are given in [19]). With increasing energy the cross section becomes similar to the one of the impulse approximation but as one sees in Fig. 3 the Argand plots remain very different.

In our opinion, the conclusions above have an important bearing on models of the  $\eta$ -nuclear interaction. In particular, they point to the fact that such models should not be developed as a mere repetition of the first-order  $\pi$ -nuclear scattering formalism.

Returning to Fig. 3 we would like to note a strong enhancement of the cross section close to zero energy as a consequence of the  $\eta^3\text{H}$  virtual state. The scattering length  $a_{\eta^3\text{H}} = (1.82 + i2.75)$  fm locates the position of the pole at  $E_{\eta^3\text{H}}^{\text{pole}} \approx -1/(a_{\eta^3\text{H}}^2 \mu_{\eta^3\text{H}}) = (1.53 + i3.59)$  MeV. The pole lies on the first nonphysical sheet ( $\mathcal{I}m\sqrt{E} < 0$ ) attached to the physical one through the two-body cut beginning at  $\eta^3\text{H}$  threshold [22]. The somewhat unusual behavior of the Argand plots near the inelastic threshold supposedly can be ascribed to a cusp-like structure of the amplitude with a rapidly varying real part.

In order to investigate the role of the short-range nucleon-nucleon dynamics we have performed in addition a four-body calculation with a Yamaguchi parametrization of the potential  $v_{NN}$  [23] where the complicated structure of the short-range  $NN$  interaction is ignored. The respective result is represented by the long-dashed curve in the Fig. 3. As one notes, the difference is insignificant. An obvious conclusion, which follows, is that in the low-energy region only the long range part of the  $NN$  interaction comes into play, which may be described quite satisfactorily by the Yamaguchi potential. In other words, our results are not sensitive to the  $NN$  interaction models (which must, of course, be on-shell equivalent at low energy) as long as the momenta in question are essentially smaller than those associated with the short-range part of the  $NN$  force.

#### IV. $\eta$ -PHOTOPRODUCTION ON A=3 NUCLEI NEAR THRESHOLD

Turning now to  $\eta$ -photoproduction, we treat the electromagnetic interaction as usual up to the first order in the fine structure constant. As a consequence, the photon appears only in the initial state as an incident particle. This scheme is illustrated in Fig. 4 where the electromagnetic vertex functions  $u^\alpha$  ( $\alpha = 2, 3$ ) are of first order in the  $\gamma N$  coupling. The corresponding expression of the amplitude  $Y_{11}^{(ss')}$  reads

$$Y_{11}^{(ss')}(p, k_\gamma; E) = \sum_{\alpha=2,3} \sum_{l,m} \sum_{\sigma=0,1} \int_0^\infty X_{\alpha 1;l1}^{(s\sigma)}(p, p'; E) \Theta_{\alpha;lm}^{(\sigma)}\left(E - \frac{p'^2}{2M_\alpha}\right) U_{1\alpha;1m}^{(\sigma s')}(p', k_\gamma; E) \frac{p'^2 dp'}{2\pi^2}, \quad (36)$$

where the hadronic amplitudes  $X_{\alpha 1}$  are defined in section II (see Eq. (5)). Here the spin coupling in the initial  $\gamma 3N$  state is also uniquely determined by the spin  $s$  of the  $NN$ -pair since the spin of the target is fixed to  $S = 1/2$ . The effective potentials, involving the photon-induced excitation of the resonance  $N^*$ , are defined by

$$U_{1\alpha;nn'}^{(ss')}(p, k_\gamma; E) = \frac{(\Omega_\alpha^{(t_\gamma)})_{ss'}}{2} \int_{-1}^{+1} v_{d;n}^{1(s)}(q_1, -\varepsilon_{3H}) \tau_d^{(s)}\left(-\varepsilon_{3H} - \frac{3q_1^2}{4M_N}\right) u_{n'}^{\alpha(ss',t_\gamma)}(q_\alpha) d(\hat{k}_\gamma \cdot \hat{p}), \quad \alpha = 2, 3, \quad (37)$$

with a relative momentum at the  $(3N) \rightarrow N + (NN)$  vertex  $\vec{q}_1 = \vec{p} + \frac{1}{3}\vec{k}_\gamma$ . The form factors  $u_n^{\alpha(ss',t_\gamma)}(q_\alpha)$  are associated with the absorption of a photon having isospin  $t_\gamma$  by a nucleon or by a nucleon pair (see Fig. 4). For the  $\gamma(NN)$  and  $\gamma N$  relative momenta  $q_\alpha$  ( $\alpha = 2, 3$ ) we use semirelativistic expressions

$$\vec{q}_2 = \vec{k}_\gamma + \frac{\omega_\gamma}{\omega_\gamma + 2M_N} \vec{p}, \quad \vec{q}_3 = \vec{k}_\gamma + \frac{\omega_\gamma}{\omega_\gamma + M_N} \vec{p}. \quad (38)$$



The spin-isospin coefficients, presented in (37) in matrix form by  $\Omega_\alpha^{(t_\gamma)}$ , are obtained from standard spin algebra

$$\Omega_2^{(0)} = \begin{pmatrix} 0 & 0 \\ 0 & 2\sqrt{\frac{2}{3}} \end{pmatrix}, \quad \Omega_2^{(1)} = \begin{pmatrix} 0 & \pm\sqrt{\frac{2}{3}} \\ \pm\sqrt{\frac{2}{3}} & 0 \end{pmatrix}, \quad \Omega_3^{(0)} = \begin{pmatrix} \sqrt{6} & 0 \\ 0 & -\sqrt{\frac{2}{3}} \end{pmatrix}, \quad \Omega_3^{(1)} = \begin{pmatrix} \mp\sqrt{\frac{2}{3}} & 0 \\ 0 & \mp\sqrt{\frac{2}{3}} \end{pmatrix} \quad (39)$$

with the upper (lower) sign referring to  ${}^3\text{He}$  ( ${}^3\text{H}$ ), respectively.

It should be noted, that going from  $\eta$  elastic scattering to  $\eta$ -photoproduction we are faced with qualitatively new physics where large momentum transfers dominate. In particular, due to this reason, the contribution of pion exchange between the nucleons to the  $\eta$  production mechanism must be included in general. This fact is confirmed by several theoretical developments [24, 25]. However, for reasons of principal numerical difficulties, already noted in Sect. II, we do not include pion rescattering into our calculation and make only several remarks in the conclusion.

As for the electromagnetic vertex functions  $u_n^\alpha$ , it is easy to show that up to the first order in the  $\gamma N$  interaction they are given by (cf. Eq. (13))

$$u_n^{\alpha(ss', t_\gamma)}(q_\alpha) = \int_0^\infty \tilde{V}_{\alpha; dN^*}^{(s, t_\gamma)}(q_\alpha, q') \tau_{N^*} \left( B_\alpha - \frac{q'^2}{2\mu_{N^*}^\alpha} \right) v_{N^*; n}^{\alpha(s')}(q', B_\alpha) \frac{q'^2 dq'}{2\pi^2}, \quad \alpha = 2, 3, \quad (40)$$

where the effective potentials  $\tilde{V}_{\alpha; dN^*}^{(s, t_\gamma)}$  are determined analogously to the hadronic potentials  $V_{\alpha; dN^*}$  [4] but with an incident  $\eta$  replaced by a photon

$$\tilde{V}_{2; dN^*}^{(s, t_\gamma)}(q_2, q') = -\frac{1}{\sqrt{2}} \int_{-1}^{+1} \frac{g_d^{(s)}(|\vec{q}' + \frac{1}{2}\vec{q}_2|) \tilde{g}_{N^*}^{(t_\gamma)}(|\vec{q}_2 + \frac{\omega_\gamma}{\omega_\gamma + M_N} \vec{q}'|, \omega_{N^*})}{\varepsilon_{3H} + \frac{3}{4M_N}(\vec{p} + \frac{1}{3}\vec{k}_\gamma)^2 + \frac{1}{M_N}(\vec{q}' + \frac{1}{2}\vec{q}_2)^2} d(\hat{q} \cdot \hat{q}'), \quad (41)$$

$$\tilde{V}_{3; dN^*}^{(s, t_\gamma)}(q_3, q') = -\frac{g_d^{(s)}(q') \tilde{g}_{N^*}^{(t_\gamma)}(q_3, \omega_{N^*})}{\varepsilon_{3H} + \frac{3}{4M_N}(\vec{p} + \frac{1}{3}\vec{k}_\gamma)^2 + \frac{1}{M_N}q'^2}, \quad (42)$$

where  $\tilde{g}_{N^*}^{(t_\gamma)}(k_{\gamma N}, \omega_{N^*})$  denotes the  $\gamma N \rightarrow N^*$  vertex functions depending on the  $\gamma N$  c.m. momentum  $k_{\gamma N}$  and the invariant  $\eta N$  energy  $\omega_{N^*}$ . The denominators in the expressions (41) and (42) are obtained by taking into account the on-shell conditions in the initial  $\gamma {}^3\text{H}$  state, i.e.  $E = -\varepsilon_{3H} + \omega_\gamma - m_\eta + k_\gamma^2/2M_{3H}$  as well as the dependence of the momenta  $\vec{q}_2$  and  $\vec{q}_3$  on  $\vec{k}_\gamma$  and  $\vec{p}$  given by (38). One readily sees that the singularities on the real  $q'$ -axis are never reached in  $\tilde{V}_{\alpha; ij}$ .

In the actual calculation, we treat the vertices  $\tilde{g}_{N^*}^{(t_\gamma)}(k, \omega_{N^*})$  independent of the momentum  $k$  and parametrize their behavior in the following form

$$\tilde{g}_{N^*}^{(1)}(k, \omega_{N^*}) = \begin{cases} \frac{e}{\sqrt{4\pi}} \sum_{n=0}^4 a_n \left( \frac{k_\pi}{m_\pi} \right)^n, & \omega_{N^*} > M_N + m_\pi, \\ \tilde{g}_{N^*}^{(1)}(k, \omega_{N^*}) \Big|_{\omega_{N^*} = M_N + m_\pi}, & \text{else,} \end{cases} \quad (43)$$

$$\tilde{g}_{N^*}^{(0)}(k, \omega_{N^*}) = 0.1 \tilde{g}_{N^*}^{(1)}(k, \omega_{N^*}),$$

where  $k_\pi$  is the on-shell pion momentum in the  $\pi N$  c.m. frame corresponding to the total energy  $\omega_{N^*}$ . The isospin separation of the  $S_{11}(1535)$  photoexcitation amplitude is chosen such that the relation

$$\frac{\sigma(\gamma p \rightarrow \eta p)}{\sigma(\gamma n \rightarrow \eta n)} = 0.67, \quad (44)$$

is reproduced in accordance with the experimental results for quasifree  $\eta$ -photoproduction on light nuclei [27, 28]. The coefficients in (43)

$$a_0 = 5.007 \cdot 10^{-1}, \quad a_1 = -1.750 \cdot 10^{-2}, \quad a_2 = 0.926 \cdot 10^{-1}, \quad a_3 = 2.052 \cdot 10^{-3}, \quad a_4 = -6.408 \cdot 10^{-3} \quad (45)$$

were obtained by fitting the  $\gamma p \rightarrow \eta p$  data [29] as shown in Fig. 5. In the same figure we also compare our calculation of the  $\gamma p \rightarrow S_{11}(1535) \rightarrow \pi p$  amplitude  ${}_p E_{0+}^{(1/2)}$  with the results of the MAID parametrization [30]. For definiteness, we present here the elementary photoproduction amplitude for  $\gamma p \rightarrow \pi p$

$$t_\lambda = {}_p E_{0+}^{(1/2)} (\vec{\sigma} \cdot \vec{\varepsilon}_\lambda) \quad \text{with} \quad {}_p E_{0+}^{(1/2)} = [\tilde{g}_{N^*}^{(0)}(k_\gamma, \omega_{N^*}) + \tilde{g}_{N^*}^{(1)}(k_\gamma, \omega_{N^*})] \tau_{N^*}(\omega_{N^*} - M_N - m_\eta) g_{N^*}^{(\eta)}(k_\eta). \quad (46)$$

The c.m. differential cross section then reads

$$\frac{d\sigma}{d\Omega}(\gamma p \rightarrow \eta p) = \frac{k_\eta}{k_\gamma} \frac{2\omega_\eta E_{N_i} E_{N_f}}{(4\pi\omega_{N^*})^2} \left| {}_p E_{0+}^{(1/2)} \right|^2, \quad (47)$$

with  $\omega_\eta$  and  $E_{N_{i(f)}}$  denoting the energies of the  $\eta$  meson and the initial (final) nucleon, respectively.

Before completing the formal part, we recall once more that all the expressions above relate only to the  $s$ -wave. With increasing energy, higher partial waves, where however no significant interaction is expected, are needed to fill the available phase space. To take into account their contribution we use here the standard prescription

$$Y = Y_{PW} + [Y - Y_{PW}]_{L=0}, \quad (48)$$

where  $Y_{PW}$  is the plane wave approximation to the production amplitude. Assuming that the hadronic interaction in the higher partial waves is insignificant, the difference in the parenthesis is reduced to  $s$ -waves only. The amplitude  $Y_{L=0}$  is given by (36). The diagrammatic representation of the amplitude  $Y_{PW}$  is presented in the Fig. 6. The corresponding analytic expression is easily obtained and need not be presented here. We note only that each term in the sum is represented by a 6-dimensional integral, which were calculated numerically without any approximation.

The reaction matrix element for the transition between the nuclear states with spin 1/2 is related to the amplitude (48) by the Wigner-Eckart formula

$$\langle \frac{1}{2} M_f | T_\lambda | \frac{1}{2} M_i \rangle = \frac{1}{\sqrt{2}} \langle \frac{1}{2} M_i \ 1\lambda | \frac{1}{2} M_f \rangle \sum_{ss'=0,1} Y^{(ss')}. \quad (49)$$

For the unpolarized c.m. cross section, we obtain

$$\frac{d\sigma}{d\Omega}(\gamma A \rightarrow \eta A) = \frac{k_\eta}{k_\gamma} \frac{2\omega_\eta E_{A_i} E_{A_f}}{(4\pi W)^2} \frac{1}{6} \left| \sum_{ss'=0,1} Y^{(ss')}(\vec{k}_\gamma, \vec{k}_\eta) \right|^2, \quad (50)$$

with  $E_{A_{i(f)}}$  being the total target energy in the initial (final) state.

Our predictions for total as well as differential cross sections are shown in Fig. 7. Firstly we note an approximate equality

$$\frac{\sigma(\gamma n \rightarrow \eta n)}{\sigma(\gamma p \rightarrow \eta p)} \approx \frac{\sigma(\gamma {}^3\text{He} \rightarrow \eta {}^3\text{He})}{\sigma(\gamma {}^3\text{H} \rightarrow \eta {}^3\text{H})} \approx 0.6. \quad (51)$$

As was already explained in [7, 26] this result is a consequence of the spin-flip nature of the  $\eta$ -photoproduction amplitude  $t_\lambda$  (46). Approximating the spatial part of the target wave function (17) by only the principal, totally symmetric  $s$ -state it is easy to see that the  $\eta$ -meson can only be produced on the neutron in  ${}^3\text{He}$  and on the proton in  ${}^3\text{H}$ . The remaining two nucleons, coupled to a total spin  $s = 0$ , do not participate due to the Pauli principle. The  $\eta$ -rescattering effects, being spin-independent do not distort this relation. A small deviation from the relation (44) is simply due to the presence of the state with mixed permutation symmetry.

As expected, the final state interaction leads to a rather pronounced enhancement of the plane wave result, especially very close to the production threshold. The cross section reaches very fast its characteristic value and has a form of a flat plateau. The angular distribution of  $\eta$ -mesons in both reactions is shown in the upper right panel of the Fig. 7. Within our model only the angular-independent  $s$ -wave part of the  $\eta 3N$  wave function undergoes distortion due to the FSI. As a consequence, the differential cross section is much more isotropic as compared with the plane wave calculation.

Comparing our results for  ${}^3\text{He}(\gamma, \eta){}^3\text{He}$  reaction with those of Ref. [7] obtained within the finite-rank-approximation (FRA), we observe rather well agreement in magnitude of the total cross sections close to the threshold (we take for comparison the results of [7] corresponding to the model IIIa for the  $\eta N$ -interaction). However we think, this fact has no physical significance, since there are principal differences in the models. Firstly, we would like to note a disagreement concerning the nature of the final state interaction. Namely, as explained in Ref. [7] the strong effect of FSI, found by the authors, is due to the  $s$ -wave  $\eta 3N$  resonance, located near zero kinetic energy [31]. In our case it

is a consequence of the virtual state, as was already discussed in [4]. We do not find any evidence for the resonance behavior of the  $\eta$   $^3\text{H}$  amplitude (see, e.g., the Argand plots in Fig. 3). Furthermore, our calculation does not exhibit a strong slope in the cross section caused by a cusp at the inelastic threshold, which was found to be very pronounced in [7].

In the lower panel of Fig. 7, we also depict the total cross section for the reaction on  $^3\text{H}$  where the final state is distorted by the first-order optical potential (the approximation denoted as DW). The corresponding photoproduction amplitude is given by (cf. Eq. (33))

$$Y(\vec{k}_\eta, \vec{k}_\gamma; E) = Y_{PW}(\vec{k}_\eta, \vec{k}_\gamma; E) + \frac{2}{3} \frac{\mu_{\eta^3\text{H}}}{\pi^2} \int_0^\infty \frac{T(k_\eta, p; E) [Y_{PW}(\vec{p}, \vec{k}_\gamma; E)]_{L=0}}{k_\eta^2 - p^2 + i\varepsilon} p^2 dp, \quad (52)$$

where the  $T$ -matrix for the  $\eta$   $^3\text{H}$  scattering  $T(k_\eta, p; E)$  was calculated with the potential (32). As one readily notes, the DW approach visibly underestimates the strong FSI effect of the four-body theory.

A comparison of the DW calculation for the reaction  $^3\text{He}(\gamma, \eta)^3\text{He}$  with the full model has also been done in [7]. In particular, the authors have noted a very large difference between the cross sections obtained within FRA and DW approaches. At the energy  $E_\gamma = 605$  MeV the DW results reported in [7] underpredict those of the FRA model by about a factor 20. The reason of this disagreement is a very strong suppression of the DW cross section in the near-threshold region. In contrast to this conclusion, our calculation predicts a typical  $s$ -wave energy dependence of the cross section for the coherent reaction of the form

$$\sigma \sim \sqrt{E_\gamma - E_\gamma^{th}}, \quad (53)$$

with  $E_\gamma^{th}$  denoting the threshold energy. This form is slightly distorted by the  $\eta$ -nuclear optical potential which tends to increase the cross section value close to the threshold. As a consequence the difference between the DW result and the full four-body calculation turns out to be not so impressive as in [7].

## V. CONCLUSION

In the present paper we have investigated elastic scattering and photoproduction of  $\eta$ -mesons on three-body nuclei near threshold. The possibility of having the exact solution at hand permits us to investigate unambiguously the corrections to the lowest-order optical potential which are usually neglected within the "standard" optical model approach. According to the results presented above, we would like to draw the following conclusions:

(i) The  $\eta N$  scattering amplitude is appreciably modified in the nuclear medium. The contributions beyond the impulse approximation turn out to be very important. It is reasonable to assume that the origin of this fact lies in the resonance nature of the  $\eta N$  amplitude giving rise to large corrections caused by the binding of the nucleons. One may expect that this effect is even stronger in heavier nuclei.

(ii) The influence of virtual target excitations between successive scatterings is also rather important. Although the three- and four-body thresholds are relatively far from the  $3N$  binding energy, neglect of the excited states makes the result very different from the exact one. In other words, the contributions of virtual three- and four-body states are also quite important below the corresponding unitary cuts.

(iii) Since in the energy region considered here the incident energy of the  $\eta$ -meson remains small, i.e., its wave-length is large compared to the characteristic internuclear distance, the results for the  $\eta$   $^3\text{H}$  scattering are not visibly sensitive to the details of the short-range  $NN$ -dynamics. This conclusion is confirmed straightforwardly comparing the results of the PEST potential [11] with those given by the simplest Yamaguchi form of the  $NN$  interaction.

(iv) Close to the threshold, the final state interaction enhances the  $\eta$ -yields appreciably, which was already noted in a variety of studies of  $\eta$ -production on lightest nuclei with different entry channels [32, 33, 34]. The angular distribution shows pronounced isotropy, associated with the  $s$ -wave dominance of FSI.

In conclusion, we would like to note once more the possible importance of pion exchange in the  $\eta$ -photoproduction on nuclei. One can expect this since the suppression due to the strong momentum transfer which is presumably important for low-energy  $\eta$   $3N$  scattering appears not to be effective here. Furthermore, as was already noted, due to the spin-flip nature of the  $\eta$ -photoproduction mechanism, only  $\approx 1/3$  of the nucleons are involved in the process. This may further enhance the importance of the  $\pi$ -exchange contribution where the nonvanishing non-spin-flip part gives rise to a coherent enhancement of the reaction strength. A good case in point is the pion production via  $\Delta(1232)$  excitation (the spin-independent part dominates) with subsequent rescattering into  $\eta$  through the excitation of  $S_{11}(1535)$  (the spin-flip part is negligible) on the next nucleon. On the other hand, we suppose that due to the short range nature of the pion-rescattering mechanism its contribution does not influence the strong energy dependence of the cross section discussed above but its magnitude can be visibly affected.

## Acknowledgments

The work was supported by the Deutsche Forschungsgemeinschaft (SFB 443).

- 
- [1] T. Ueda, Phys. Rev. Lett. **66**, 297 (1991), Phys. Lett. B **291**, 228 (1992).
  - [2] C. Wilkin, Phys. Rev. C **47**, R938 (1993).
  - [3] S. Wycech, A.M. Green, J.A. Niskanen, Phys. Rev. C **52**, 544 (1995).
  - [4] A. Fix and H. Arenhövel, Phys. Rev. C **66**, 024002 (2002).
  - [5] M. Ericson and T.E.O. Ericson, Ann. Phys. **36**, 323 (1966).
  - [6] M. Pfeiffer, Ph.D. Thesis (Giessen 2002).
  - [7] N.V. Shevchenko *et al.*, Nucl. Phys. A **699**, 165 (2002).
  - [8] S.A. Sofianos, N.J. McGurk, and H. Fiedeldey, Nucl. Phys. A **318**, 295 (1979).
  - [9] A. C. Fonseca, Proc. 8th Autumn School on Models and Methods in Few-Body Physics, Lisboa, 1986, eds. L.S. Ferreira, A.C. Fonseca and L. Streit, Lecture Notes in Physics **273**, 161 (1986).
  - [10] There are separable expansion methods, which seem to be capable of approximating the three-body off-shell scattering amplitudes also at positive energies (see e.g. A.C. Fonseca, H. Haberzettl, and E. Cravo, Preprint BONN-HE-82, July 1982). But they require far more numerical efforts and were not adopted here.
  - [11] H. Zankel, W. Plessas, and J. Haidenbauer, Phys. Rev. C **28**, 538 (1983).
  - [12] Q. Haider and L.C. Liu, Phys. Rev. C **66**, 045208 (2002).
  - [13] C. Bennhold and H. Tanabe, Nucl. Phys. A **530**, 625 (1991).
  - [14] R.A. Arndt, J.M. Ford, and L.D. Roper, Phys. Rev. D **32**, 1085 (1985).
  - [15] M. Batinić, I. Šlaus, A. Švarc, and B.M.K. Nefkens, Phys. Rev. C **51**, 2310 (1995).
  - [16] M.L. Goldberger and K.M. Watson, *Collision Theory* (Wiley, N.Y., 1964).
  - [17] A.K. Kerman, H. McManus, and R.M. Thaler, Ann. Phys. (N.Y.) **8**, 551 (1959).
  - [18] R. Aaron, R.D. Amado, and Y.Y. Yam, Phys. Rev. **136**, B650 (1964).
  - [19] S. Wycech and A.M. Green, Phys. Rev. C **64**, 045206 (2001).
  - [20] H.P. Noyes, Phys. Rev. Lett. **15**, 538 (1965); K.L. Kowalski, Phys. Rev. Lett. **15**, 798 (1965).
  - [21] R.S. Hayano, S. Hirenzaki, and A. Gillitzer, Eur. Phys. J. A **6**, 99 (1999).
  - [22] More exactly, there are two poles which are placed symmetrically about the real energy axis.
  - [23] Y. Yamaguchi, Phys. Rev. **95**, 1628 (1954).
  - [24] L.C. Liu, Phys. Lett. B **288**, 288 (1992).
  - [25] F. Ritz and H. Arenhövel, Phys. Rev. C **64**, 034005 (2001).
  - [26] L. Tiator, C. Bennhold, and S.S. Kamalov, Nucl. Phys. A **580**, 455 (1994).
  - [27] P. Hoffmann-Rothe *et al.*, Phys. Rev. Lett. **78**, 4697 (1997).
  - [28] V. Hejny *et al.*, Eur. Phys. J. A **6**, 83 (1999).
  - [29] B. Krusche *et al.*, Phys. Rev. Lett. **74**, 3736 (1995).
  - [30] D. Drechsel, O. Hanstein, S.S. Kamalov, and L. Tiator, Nucl. Phys. A **645**, 145 (1999).
  - [31] V.B. Belyaev, S.A. Rakityansky, S.A. Sofianos, M. Braun, and W. Sandhas, Few Body Syst., Suppl. **8**, 309 (1995); S.A. Rakityansky, S.A. Sofianos, M. Braun, V.B. Belyaev, and W. Sandhas, Phys. Rev. C **53**, R2043 (1996).
  - [32] B. Mayer *et al.*, Phys. Rev. C **53**, 2068 (1996).
  - [33] H. Calen *et al.*, Phys. Rev. Lett. **79**, 2642 (1997).
  - [34] V. Hejny *et al.*, Eur. Phys. J. A **13**, 493 (2002).

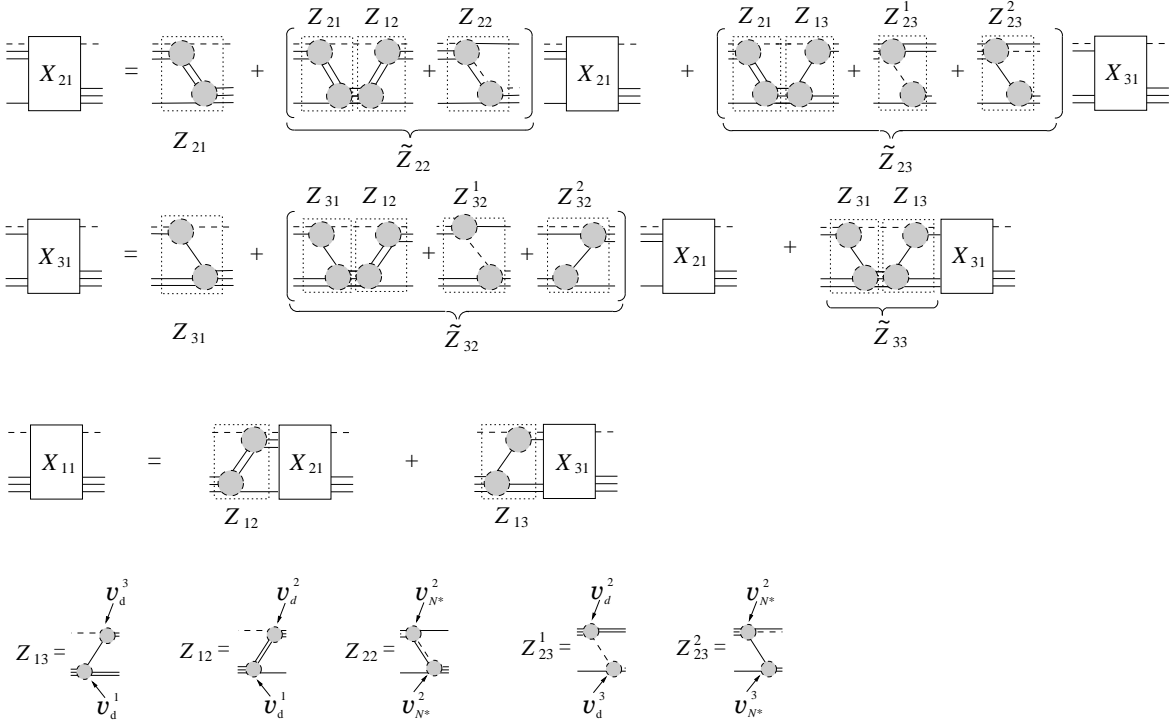


FIG. 1: Diagrammatic representation of the coupled integral equations (5) and (9) for the  $\eta 3N$  scattering and the effective potentials  $Z_{\alpha\beta}$  and  $\tilde{Z}_{\alpha\beta}$ . The dashed line represents an  $\eta$ -meson. The lines close together indicate different two- and three-body quasiparticles.

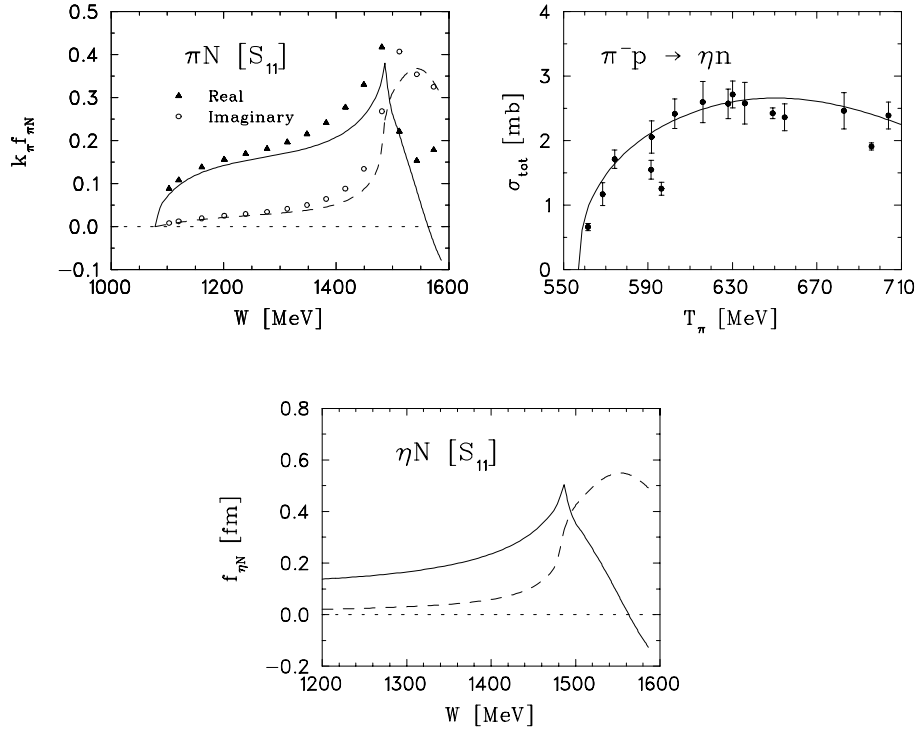


FIG. 2: Upper left panel: the  $S_{11}$  partial wave of the  $\pi N$  scattering amplitude predicted by the parametrization of  $S_{11}(1535)$  resonance used in the present paper (see Eq. (22) and (24)). Notations: solid curve: real part, dashed: imaginary part. Circles and triangles represent the result of the VPI-analysis [14]. Upper right panel: total  $\pi^- p \rightarrow \eta n$  cross section. The data are taken from the compilation presented in [15]. Lower panel: the  $\eta N$  off-shell scattering amplitude  $f_{\eta N}(\vec{q}, \vec{q}'; W)$  at  $q = q' = 0$ . Notations as in the upper left panel.

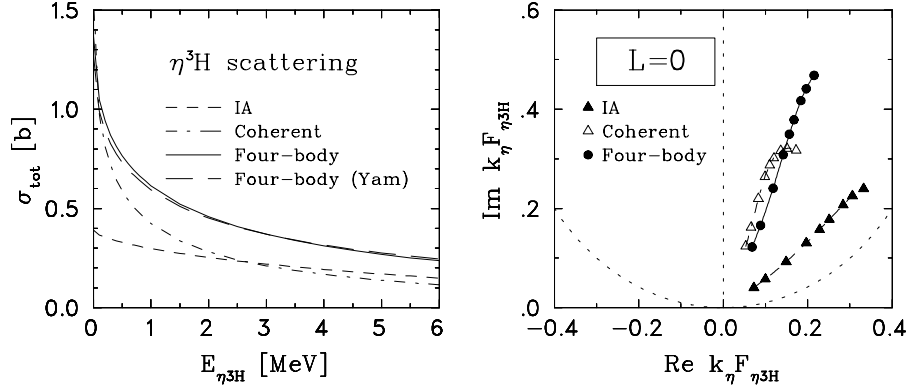


FIG. 3: Elastic cross section for  $\eta^3\text{H}$  scattering (left panel) and Argand plot (right panel) of the scattering amplitude. The dashed curves (filled triangles on the right panel) represent the impulse approximation to the first-order optical potential (Eq.(32)). In the dash-dotted curves (open triangles) the medium corrections to the single scattering are taken into account (Eq.(30)). The solid curves (filled circles) represent the result of the full four-body calculation. The long-dashed curve in the left panel is obtained with the Yamaguchi  $NN$ -potential embedded into the nuclear sector. In the right panel the circles and triangles indicate the following c.m. kinetic energies :  $E_{\eta^3\text{H}} = 0.1, 0.2, 0.5, 1.0, 1.5, 2.0, 3.0, 4.0,$  and  $6.0$  MeV.

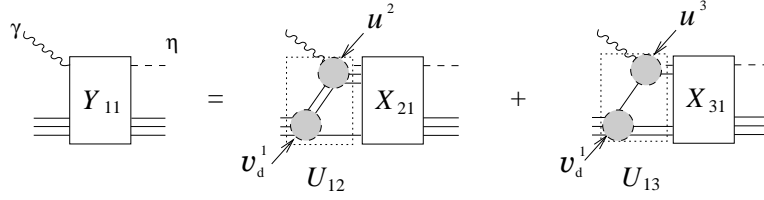


FIG. 4: The photon induced effective potentials appearing in leading order of the electromagnetic interaction in  $\eta$ -photoproduction on three-body nuclei (37).

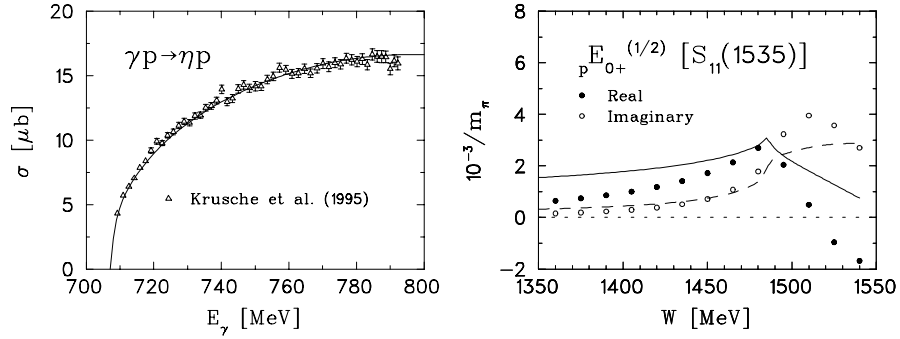


FIG. 5: Left panel: the  $\gamma p \rightarrow \eta p$  total cross section compared with the data of [29]. Right panel: the  $pE_{0+}^{(1/2)}$  multipole of  $\gamma p \rightarrow \pi p$  generated by the photoexcitation of the  $S_{11}(1535)$  resonance. Solid curve: real part, dashed curve: imaginary part. Open and filled circles represent the results of the MAID-parametrization [30].

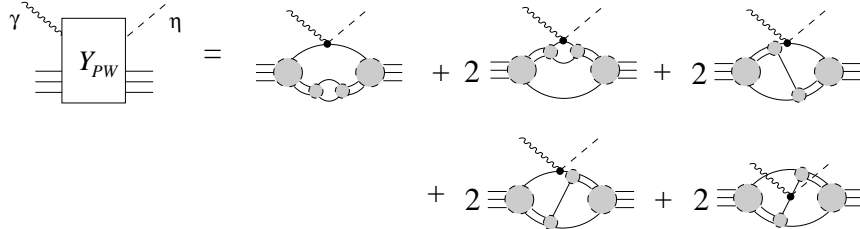


FIG. 6: Schematic representation of the PWIA-term in the  $\eta$ -photoproduction amplitude (48) related to our model of the target wave function (17)-(18). The factors 2 stem from the identity of the nucleons.

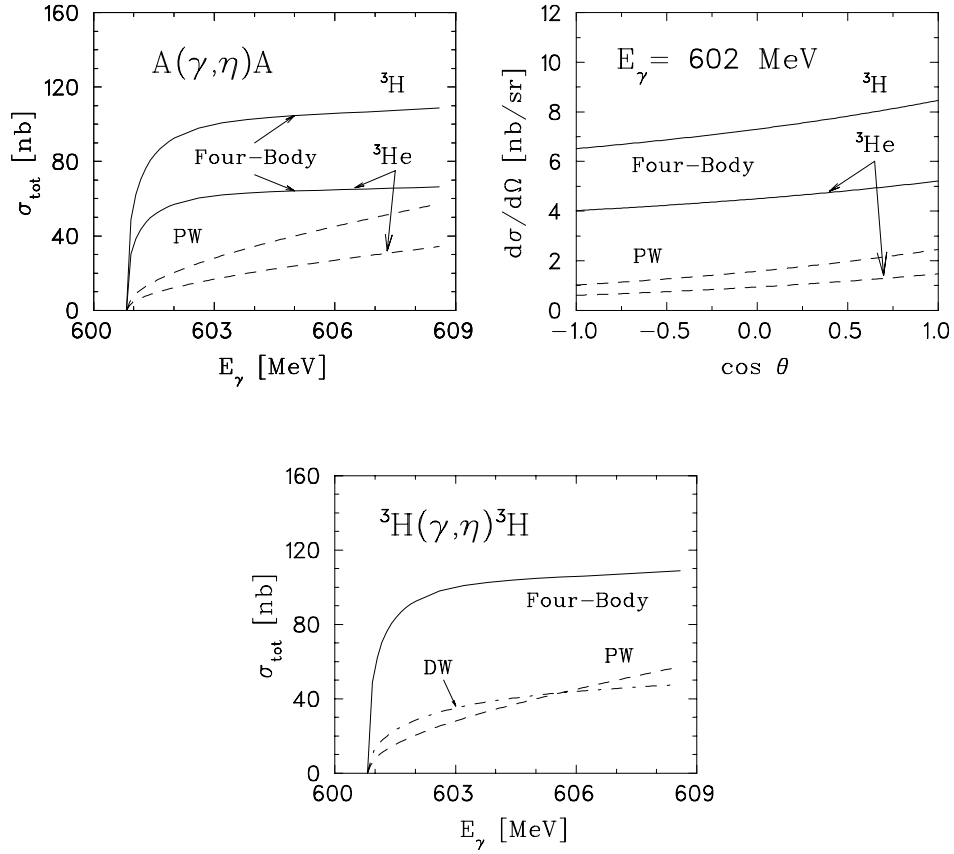


FIG. 7: Upper panels: total and differential cross section for  $\eta$ -photoproduction on  ${}^3\text{He}$  and  ${}^3\text{H}$  calculated within the four-body scattering model for the final  $\eta 3N$  system compared to the results of the plane-wave calculation (the dashed curves on both panels). In the lower panel the FSI effects provided by the distorted wave (DW) approach with the optical potential (32) (dash-dotted curve) are compared with those given by the four-body calculation and the plane-wave approximation (PW).